

Enhanced Electrical Conductivity of Highly Crystalline Polythiophene/Insulating-Polymer Composite

Guanghao Lu, Haowei Tang, Yunpeng Qu, Ligui Li, and Xiaoni Yang*

State Key Laboratory of Polymer Physics and Chemistry, Changchun Institute of Applied Chemistry, Chinese Academy of Sciences, Graduate School of the Chinese Academy of Sciences, Renmin Str. 5625, Changchun 130022, P.R. China

Received May 20, 2007; Revised Manuscript Received June 29, 2007

ABSTRACT: Poly(3-butylthiophene) (P3BT)/insulating-polymer composites with high electrical conductivity have been prepared directly from the solution. These composites exhibit much higher conductivity compared to pure P3BT with the same preparation method provided that P3BT content is higher than 10 wt %. Morphological studies on both the pure P3BT and the composites with insulating polymer show that P3BT highly crystallizes and develops into whisker-like crystals. These nanowires are homogeneously distributed within the insulating polymer matrix and form conductive networks, which provide both extremely large interface area between conjugated polymer and insulating polymer matrix and highly efficient conductive channels through out the whole composite. In contrast, the conductivity enhancement of P3HT/PS composite is not so obvious and drops down immediately with increased PS content due mainly to the absence of highly crystalline whisker-like crystals and much larger scale phase separation between the components. The results presented here could further illuminate the origin of conductivity formation in organic semiconducting composites and promote applications of these polymer semiconductor/insulator composites in the fields of organic (opto-)electronics, electromagnetic shielding, and antistatic materials.

Introduction

Conjugated polymers have great potentials in many applications such as light-emitting diodes,^{1,2} thin film transistors,^{3,4} polymer solar cells,^{5,6} and conductive coating.^{7,8} As an important member in the family of conjugated polymers, poly(3-alkylthiophene) (P3AT)⁹ has been intensively studied for its applications in such as polymer-based field-effect transistors,⁴ polymer solar cells,^{6,10} electromagnetic compatible materials,⁸ and so on. However, the expensive price and low stability of P3AT prevents its large-scale application and potential expansions in the other fields. The focus are thus diverted to the composites^{11–13} consisting of polythiophene and insulating polymers so as to reduce cost, improve stability via self-encapsulant,¹³ and increase mechanical properties. Although recently a few results have shown that the charge carrier mobility retains almost the same in the composite of poly(3-hexylthiophene) (P3HT) and crystalline insulating polymer within a rather wide ratio between the two components compared to the pure P3HT,¹¹ the composite with higher conductivity than corresponding pure polythiophene has not been reported yet. Additionally, the phase organization of conductive and insulating components in the composite, in particular, the length-scale of phase separation, is of fundamental importance to the conductivity behaviors of the whole composite.^{11,13} In this work, by manipulating the organization of each phase in the composite, we demonstrate that conductivity of the composite can be enhanced upon mixing highly crystallized poly(3-butylthiophene) (P3BT) with insulating polymers such as amorphous polystyrene (PS) or poly(methyl methacrylate) (PMMA). The P3BT/PS composite with conductivity of nearly an order of magnitude higher than that of pure P3BT is achieved without any doping.

Experimental Section

Materials. Regioregular poly(3-butylthiophene) (P3BT) (97% head-to-tail regiospecific conformation, $M_w = 39.4$ kDa, PDI = 2.29) and regioregular poly(3-hexylthiophene) (P3HT) (98.5% head-to-tail regiospecific conformation, $M_w = 58.5$ kDa, PDI = 2.23) were purchased from Rieke Metals, Inc. Polystyrene (a-PS, GPPS-200D) was purchased from DaQing Petro Chemical Company and was further purified upon being dissolved in chloroform and precipitated by ethanol. *O*-dichlorobenzene (ODCB, anhydrous, 99%) was purchased from Sigma-Aldrich Co.

Sample Preparation. P3HT and PS were dissolved in solvent ODCB respectively by stirring overnight. For P3BT, slightly elevated temperature 80 °C during stirring was used to achieve a solution with concentration 10 mg/mL in ODCB. After cooling to room temperature, the solution was placed in dark and vibrationless environment to allow P3BT molecules to crystallize/self-organize in solution for 72 h. The polythiophene (P3BT or P3HT) solution was then mixed with PS solution to prepare polythiophene/PS mixed solution with different ratios. To obtain homogeneous thin film for morphology investigations, for instance X-ray diffraction (XRD) and transmission electron microscopy (TEM), polythiophene or polythiophene/PS solution was spin-coated (Laurell Spin Processor WS-400B 6NPP Lite) onto silicon wafer pretreated with standard substrate cleaning procedure for device fabrication, i.e., the substrates were first cleaned by ultrasonic treatment in acetone, rinsed in demineralized water, and refluxed with isopropanol to remove water, and finally, the substrates were treated in an UV-ozone oven for ca. 20 min.

Characterizations. For conductivity measurement, P3AT or P3AT/PS solution was cast on precleaned glass to get a comparable thickness (~4 μm). 4-probe and 2-probe methods using Keithley 2400 SourceMeter and Keithley 2000 MultiMeter were employed respectively for conductivity determination in air. The conductivity measurements based on both 2-probe and 4-probe methods were calculated from Ohm's law:

$$\sigma = Il/Va$$

Here, I , l , V , and a represent the current injected, length between the electrodes, voltage read out, cross area of film, respectively.

* Corresponding author. E-mail: xnyang@ciac.jl.cn.

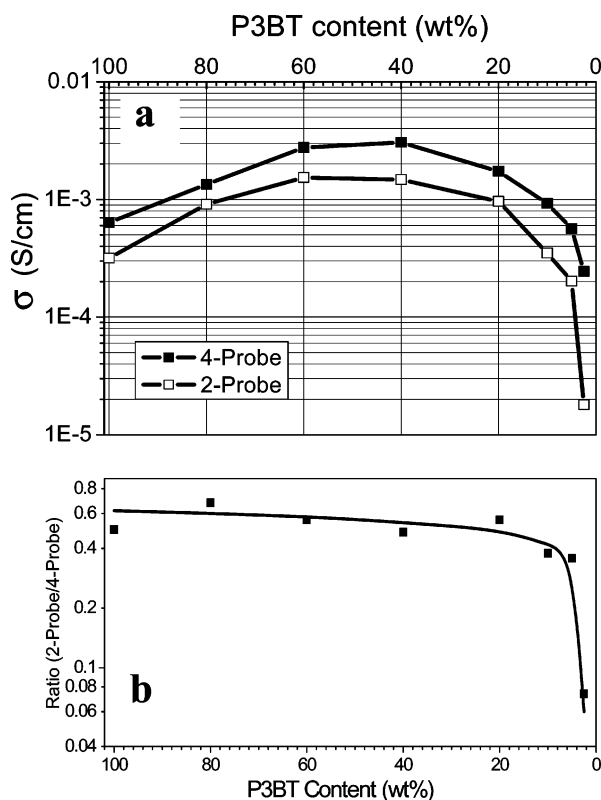


Figure 1. (a) Dependence of P3BT/PS conductivity on P3BT content in the composites as measured with a 4-probe method (solid square) and a 2-probe method (open square), respectively. (b) Difference of the results from these two methods as represented by the ratio of the measured values between the 2-probe and 4-probe methods.

Wide-angle X-ray diffraction (WAXD) profiles were obtained by using Bruker D8 Discover Reflector with X-ray generation power of 40 kV tube voltage and 40 mA tube current. The diffraction was recorded at a θ - 2θ symmetry scanning mode with scan angle 2θ within the range of 5 – 30° .

TEM was performed on a JEOL JEM-1011 transmission electron microscope operated at 100 kV. Thin films were first floated on deionized water, and then transferred onto copper grids. The samples were dried at room temperature for 24 h before TEM experiments.

Optical microscopy (OM) images were recorded on an Olympus BX51 system microscope.

Atomic force microscopy (AFM) measurements (thickness and topographic images) were performed on SPA300HV with an SPI 3800 controller Seiko Instruments Industry, Co., Ltd., and images were recorded with intermediate-contact mode at room temperature.

UV-vis measurements were carried out using Perkin-Elmer UV-vis Lambda 750 spectrometer with 1.0 nm slit width.

Results and Discussion

As shown in Figure 1, the pure P3BT film cast from its solution reaches a conductivity of 3×10^{-4} to 6×10^{-4} S/cm, depending on the method (4-probe or 2-probe) used, which is a high conductivity for nondoped P3AT.^{14–16} For comparison, the conductivity of regioregular poly(3-hexylthiophene) (P3HT) film deposited also from its ODCB solution is measured and a value in an order of only 10^{-5} S/cm is obtained in the same condition (Figure 6). Figure 1 also shows the conductivities of P3BT/PS composites with various ratios between the two components. The most exiting information coming from these results is the substantially increased conductivity, e.g., by a maximum factor of 5–8, reaching 2×10^{-3} to 3×10^{-3} S/cm upon mixing with insulating PS compared to the pure P3BT. Moreover, the conductivity of P3BT/PS with 10 wt % P3BT

content is still comparable with that of pure P3BT. The inconsistency of the results obtained from the two methods (2-probe and 4-probe), which is mainly resulted from the contact resistance at the interfaces of the probes, does not obviously increase until P3BT content reaches 5 wt %, implying that the inclusion of insulating PS into P3BT have not introduced additional contact resistance that much as long as the content of P3BT is still above this critical point. For the composite with very low P3BT content, the conductivity substantially drops down, particularly for those results determined from a 2-probe method. In this situation, contact resistance turns to be highly significant for conductivity of the P3BT/PS composite obtained.

Similar results could be also observed for P3BT/PMMA composite in our experiments, i.e., the conductivity of P3BT is enhanced upon mixing with another insulating polymer PMMA, reaching 10^{-3} S/cm (see Supporting Information Figure S1). It should be noted that in order to exclude this result from the effect of some possible impurities in PS or PMMA, very pure PS sample for gel permeation chromatography (GPC) calibration experiment has been tried and the results obtained are comparable.

To disclose this enhanced conductivity of P3BT/PS composite film, the pure P3BT in both solution and corresponding film is studied. The obvious changes of P3BT/ODCB solution from lovely orange appearance as-prepared at elevated temperature to a viscous dark solution after cooled to room temperature and kept for several hours hints the already self-organization/crystallization of P3BT in the solution. The thin P3BT film spin-coated from this viscous solution demonstrates very high crystallinity, as implied by UV-vis spectrum (Figure 2d) and the absence of amorphous halo around $2\theta^{17}$ in the WAXD profile given in Figure 2c.^{9,17} The main UV-vis absorption peak of P3BT only slight blue-shift upon blending with PS. One possible reason for this blue-shift is that during solidification from ODCB solution, those nonaggregated fraction of P3BT does not fully crystallized at the presence of PS. TEM image (Figure 2a) shows this film is mainly composed of very long whisker-like crystals with typical width of 10–20 nm and length more than 10 μ m. Actually, whisker-like appearance is a frequently obtained morphology of P3AT deposited from the solution,^{18–20} and its typical width and thickness are 10–20 nm and 3–5 nm, respectively,^{18,20} as also confirmed by AFM topography shown in Figure 2b. It has been proved that P3AT whisker-like crystal is an effective one-dimensional charge carrier transport channel,²¹ acting as an electrically conductive nanowire. Because of the limited solubility of P3BT in ODCB at room temperature, the cooling down of the prepared hot P3BT/ODCB solution gradually results in the crystallization/self-organization of P3BT in situ the solution.^{18,22} Thanks to their unique long and very thin morphology, these whisker-like P3BT crystals are stable as suspension in the solution even for several months rather than precipitate from the solution.

Upon addition of PS into P3BT solution, the crystallinity of the film in terms of the whole P3BT/PS composite decreases. For instance, the crystallinity of a composite with weight ratio of 1:1 between the components is below 50%, as shown by WAXD profile in Figure 3, the amorphous halo becomes pronounced due to the inclusion of the noncrystalline PS phase into the composite. With respect to the morphology of the composite from macroscale to nanoscale, these P3BT/PS composites show similar feature and phase evolution behaviors. Therefore, we use the composite with the ratio of 1:1 as an example to show the typical morphology of these composites. As indicated by optical microscopy image shown in Figure 4a,

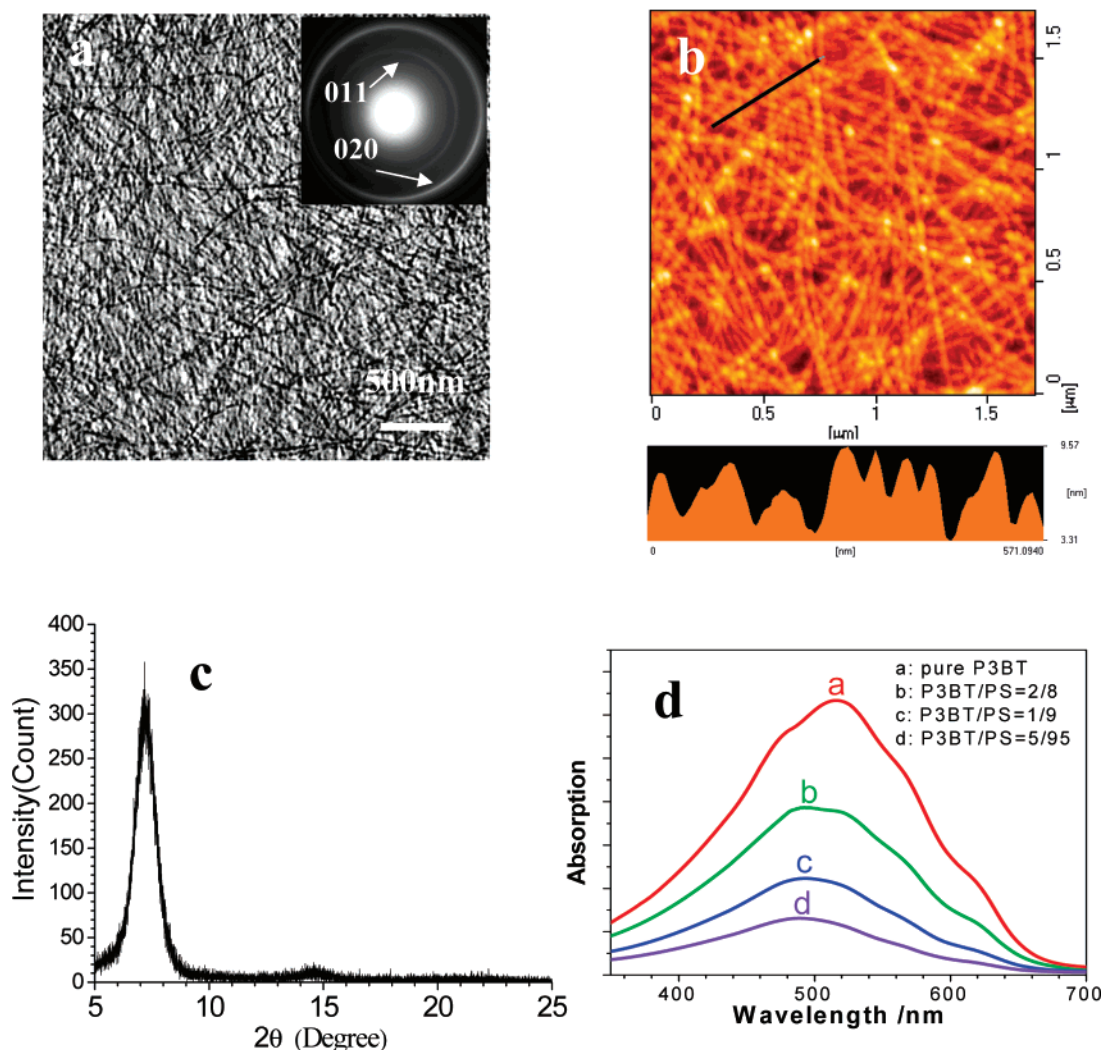


Figure 2. (a) BF-TEM image (inset is the electron diffraction pattern) and (b) AFM topography showing the highly crystalline whiskers of P3BT; (c) WAXD profile confirming the high crystallinity of P3BT in the thin film due to the absence of amorphous halo; (d) UV-vis spectrum of the thin film with different P3BT/PS ratios. All the samples are prepared from P3BT/ODCB or P3BT-PS/ODCB solution with already formed ordered aggregations via spin-coating.

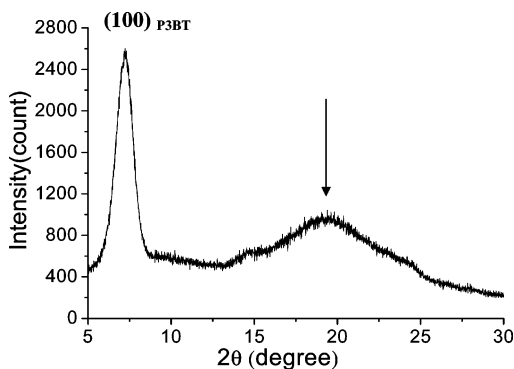


Figure 3. WAXD profile of P3BT/PS (50% P3BT) composite film cast from ODCB solution. The arrow indicates the amorphous halo of PS.

the whole P3BT/PS composite film cast appears homogeneous and featureless. The color of the film is similar to that of the pure P3BT, which hints the addition of PS into P3BT solution does not significantly change the one- or two-dimensional conjugated length of P3BT crystals. The homogeneity of the composite film at low magnification is independent of ratio between the components and the film deposition method applied. At higher magnification by using TEM, as shown in Figure 4,

parts b and c, the obtained images demonstrate whisker-like morphology which is similar to the pure P3BT film. Strikingly, these P3BT nanowires form an interconnected network within the PS matrix, without obvious aggregation. It is reasonable to conclude that these super-long P3BT nanofibers contributed to the enhanced conductivity.

The charge carrier mobility of the composite consisting P3HT and insulating polymers such as polyethylene and PS^{11,12} has been studied. It has been confirmed that the concentration of conjugated polymer in semiconductor/crystalline insulator composite can be reduced to a low value without degradation of field-effect carrier mobility.¹¹ Interestingly, the carrier mobility of P3HT/PS composite is larger than P3HT/semiconducting polymer composite, for example, P3HT/Poly[2-methoxy-5-(2-ethylhexoxy)-1,4-phenylenevinylene] (MEH-PPV), P3HT/poly(3-decylthiophene) (P3DT), and P3HT/poly(9,9-dioctylfluorene) (PFO) with the same blending ratio in a wide P3HT content range.¹² Our work also indicate that the conductivity of P3BT/P3HT composite (including the P3BT/random-P3HT composite as shown in Figure S3, which has a similar morphology when compared to the P3BT/PS composite) is obviously lower than that of pure P3BT, P3BT/PMMA, and P3BT/PS blends with the same ratio within a wide P3BT content range. Although the role of the insulating polymer is still not very clear, previous

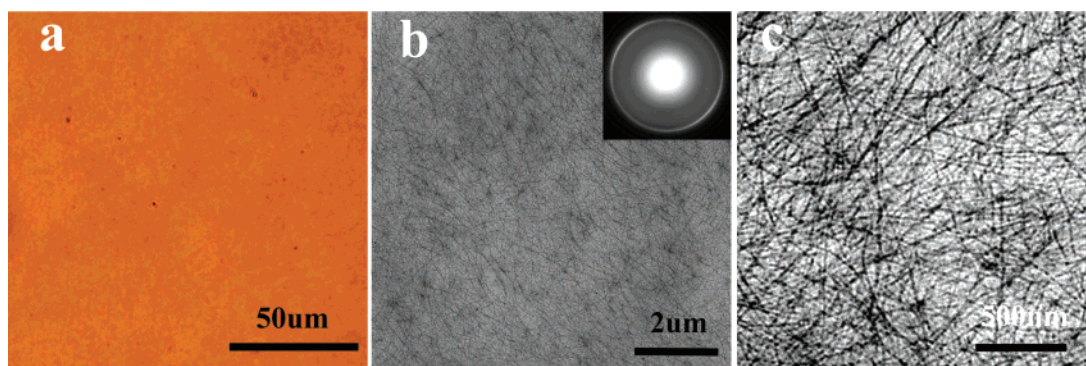


Figure 4. Morphology of P3BT/PS composite film with 50 wt % P3BT content from ODCB solution with already formed aggregations: (a) optical microscopy image; (b, c) BF-TEM images at different magnifications. The inset in part b is an electron diffraction pattern.

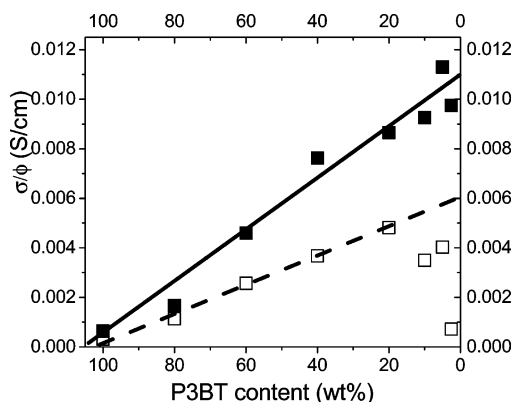


Figure 5. Dependence of σ/ϕ on P3BT content (ϕ) in the composites as measured with 4-probe method (solid square) and 2-probe method (open square), respectively. The solid line is the linear fit for the data obtained from 4-probe method within the whole P3BT range, and the dashed line is the linear fit for those data from the 2-probe method with P3BT content higher than 20 wt % content.

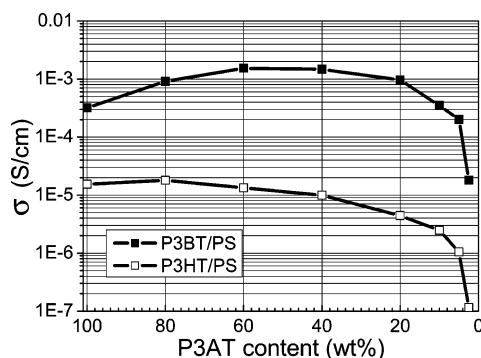


Figure 6. Dependence of polythiophene/PS conductivity on polythiophene content in the composites as measured with a 2-probe method.

work has ascribed these intriguing results to the dipolar effects arising from the polarity of the components.^{12,23,24} Recently some efforts have been paid to organic thin film and single-crystal field-effect transistor (FET) based on low permittivity dielectric layer. Consequently, enhanced device performance namely increased charge carrier mobility, reduced threshold voltage and lower hysteresis was achieved, which is opposed to the existing trend to increase the permittivity for low operational voltage.^{25,26} For example, the charge carrier mobility in the field-effect transistors based on rubrene single-crystal systematically decreases with increased dielectric constant of the gate insulator, and the amplitude of this reduction is proportional to the reciprocal of the permittivity of the dielectric layer ϵ^{-1} .²⁷

The dielectric constant ϵ of the insulating polymers used here is rather low (ϵ_{PS} , $\epsilon_{\text{PMMA}} \sim 2.5\text{--}3.5$). Actually, the values of

σ/ϕ (where σ the conductivity of the composite, and ϕ the polythiophene content (weight fraction) in the composite) should reflect the true conductivity contribution related to the P3BT nanowires in insulating polymer matrix. Figure 5 shows the dependence of σ/ϕ of P3BT/PS on P3BT content (ϕ). The data obtained from 4-probe method could be linearly fitted throughout the whole content range, while the data from 2-probe method can only be linearly fitted as the P3BT content is higher than 20%, as shown in Figure 5. The loss of linear relationship at lower P3BT content should be ascribed to the much higher interface resistance at the probes for 2-probe method. The extrapolation of σ/ϕ to $\phi = 0$, namely the intercept with the Y-axis could be used to describe the conductivity of P3BT individually dispersed in PS matrix provided that the P3BT nanowires are still interconnected with each other. Correspondingly, $(\sigma/\phi)_{\phi \rightarrow 0} = 0.011$ S/cm for 4-probe method and $(\sigma/\phi)_{\phi \rightarrow 0} = 0.006$ S/cm for 2-probe method, are ca. 17 times (4-probe method) and 19 times (2-probe method) higher than that of pure P3BT. It can be carefully concluded that for an individual conducting P3BT nanowire, the surrounding matrix indeed plays an important role in the charge carrier transport.²⁶ The conductivity of a single P3BT nanowire in PS matrix is thus at least 1 order of magnitude higher than that of P3BT nanowire in its own P3BT matrix. In this regard, it is of no ambiguity that for a wide P3BT content range the conductivity of P3BT/PS composite is obviously higher than that of P3BT/P3HT composite or pure P3BT since the polarizability of the polythiophene is much higher than that of insulating polymer PS or PMMA.¹² However, the increased conductivity of P3BT can only be attributed to enhanced charge carrier mobility since the charge carriers concentration in P3BT nanowires is at least not increased. As discussed above that interface between semiconductor and low permittivity insulator can significantly enhance charge carrier mobility of semiconductor, the homogeneously dispersed P3BT nanowires in PS matrix provides extremely large interface area between P3BT and PS, which is crucial for the increased conductivity of P3BT/PS composite in macroscopic scale.

To investigate the detailed mechanism of enhanced conductivity in P3BT/non-conjugated polymer composites, the blend consisting of another P3AT, P3HT and PS was studied. For P3HT/PS with low P3HT content (<20 wt %), it is difficult to inject the specific current for 4-probe measurement due to the too high interface resistance, so only 2-probe data is given for this case. As also shown in Figure 6, the conductivity of P3HT/PS blend gradually falls as P3HT content decreases. For P3HT/PS deposited from solution, more complicated phase behaviors have been reported and found to be sensitive to the ratio between the components.¹² For instance, for those P3HT/PS composites

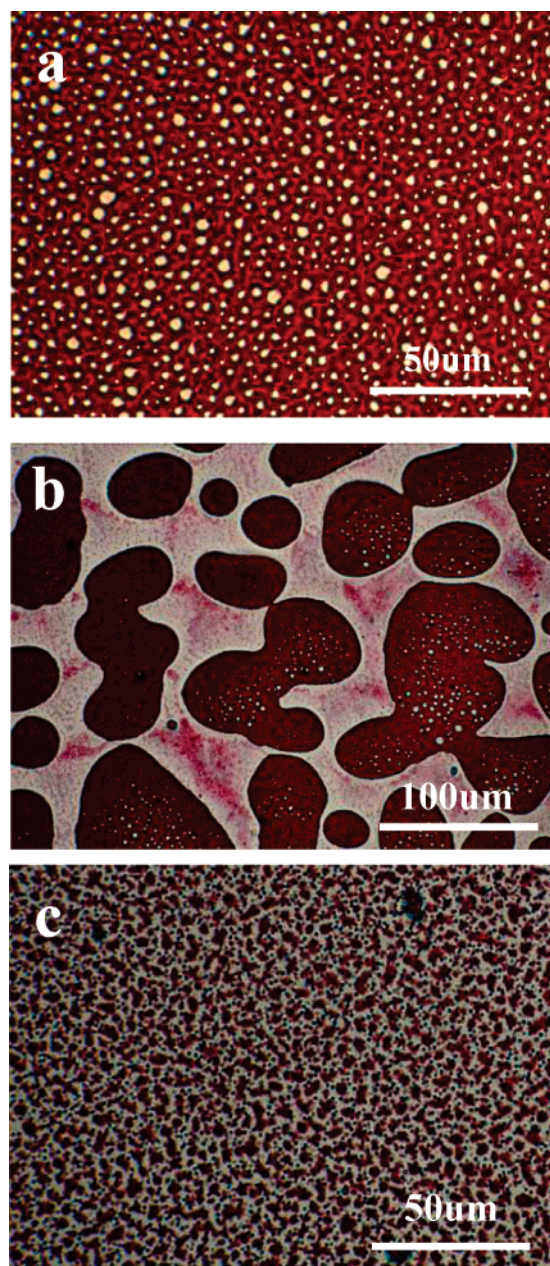


Figure 7. Optical microscopy images show the morphology of P3HT/PS composite films with different ratios (weight percent of P3HT) deposited from ODCB solution: (a) 80%, (b) 60%, and (c) 10%.

with either high or low P3HT content, they typically form a morphology that the minor component domains dispersed within matrix composed of major phase. For the composites with comparable P3HT and PS content, large-scale phase separation occurs as a result of spinodal decomposition.¹² Figure 7 shows the morphology of P3HT/PS film deposited from ODCB under the same condition for P3BT/PS composite preparation. In the case of higher ratio of 80 wt % P3HT in the composite as shown in Figure 7a, isolated droplet-like polystyrene domains are embedded in P3HT matrix. Large scale phase separation between P3HT and PS occurs as a result of spinodal decomposition at the comparable ratio between the two components (Figure 7b). In the case of very lower ratio of 10 wt % P3HT in the P3HT/PS composite, the minor component P3HT turns to be the dispersed phase, homogeneously distributing within the PS matrix (Figure 7c). Because of this strong incompatibility between the components, the phase behavior of the blends turns to be complicated and the morphology of the P3HT/PS film

obtained is almost out of control since it is highly sensitive to composition and deposition conditions, in contrast to the P3BT/PS composite.

Upon comparing the results between P3BT/PS and P3HT/PS composites in terms of conductivity and morphology, it is reasonable to relate the difference in conductivity of the composites to their striking differences in the morphology. So it is proposed that there are two competing factors ultimately determining the electrically conductive performance of P3AT/insulator composite: (1) the presence of insulator can intrinsically enhance the conductivity of P3AT; (2) large scale phase segregation however significantly deteriorates the conductivity. The eventual conductivity is the tradeoff of these two factors. Correspondingly, forming conductive P3AT network within insulator matrix will benefit the conductivity improvement, in particular for those composites with low P3AT content. Additionally, due to the strong relation between the charge carrier mobility and the crystalline order of organic semiconductor, the conductivity of P3AT/insulating-polymer composite is ultimately dependent on both the crystallinity of P3AT itself and the morphology of the composite film. However, it is difficult to achieve P3HT/PS film with simultaneously high P3HT crystallinity and small-scale phase separation due to the strong phase separation tendency at the condition which could increase crystallinity of P3HT.^{20,28}

Actually, similar to above-mentioned P3HT/PS composite, the P3BT/PS is also a thermodynamically incompatible blend system. However, due to the already presence of very long whisker-like P3BT crystals in P3BT/PS solution, these highly crystalline P3BT nanowires can be easily preserved during film deposition. Since these whisker-like crystals are quite bulky compared to polymer or other small molecules, it is impossible for them to aggregate together to undergo a large-scale phase separation driven by their thermodynamic incompatibility. In this case, the morphology of the P3BT/PS composite film is almost independent of the film deposition conditions since entangled P3BT nanowires with low diffusibility are not able to aggregate even under very slow solvent evaporation. P3BT nanowires are thus homogeneously dispersed in insulating PS matrix and form an interconnected network so as high conductivity is achieved.

Percolation theories are usually applied to describe the conducting behavior of composites composed of conductive filler and an insulator matrix. The aspect ratio (length to diameter) of the filler is a crucial factor to effectively reduce the percolation threshold for conductivity.^{29,30} Obviously, in this work the already formed whisker-like P3BT crystals in the solution is a key element to the enhanced conductivity of P3BT/PS composite. It is also due to the extremely high aspect ratio nature of these P3BT nanowires, the percolation threshold for the conductor/insulator composite substantially decreases so as the composite with only 2.5 wt % P3BT could still achieve conductivity in an order of 10^{-4} S/cm. This behavior is similar to the conductive composite prepared by introducing a small amount of carbon nanotubes into insulating polymers.³¹

Conclusion

In summary, we have shown the polythiophene/insulating-polymer composites with enhanced electrical conductivity through a crystallization/self-assembly process in the solution. Highly crystalline whisker-like P3BT crystals are first constructed in the solution together with PS. These preserved P3BT nanowires during film deposition are homogeneously dispersed and form interconnected network within insulating PS matrix,

which contributes to the enhanced conductivity. Because of the extremely large interface area between the conjugated polymer and insulating polymer matrix, the conductivity of P3BT/PS composite is enhanced to nearly an order of magnitude higher than that of pure P3BT. The negligible conductivity enhancement and drops down immediately with increased PS content in P3HT/PS composite is due mainly to the absence of highly crystalline whisker-like crystals and much larger scale phase separation between the components. The results presented here could further illuminate the origin of conductivity formation in organic semiconducting composites. The method introduced in this work could be further developed to fabricate high-conductive, long lifetime and mechanically stable materials for the applications in such as organic (opto-)electronics, electro-magnetic shielding and antistatic materials.

Acknowledgment. This work was supported by the National Natural Science Foundation of China (Grant No. 20604029) and the National Fundamental Research Specific Foundation of China (Grant No. 2005CB623800). X.Y. would like to thank the Fund for Creative Research Groups (Grant No. 50621302) for financial support.

Supporting Information Available: Figures showing the dependence of P3BT/PMMA conductivity on P3BT content and the dependence of σ/φ of P3BT/PMMA composite on P3BT content (φ) in the composites. This material is available free of charge via the Internet at <http://pubs.acs.org>.

References and Notes

- (1) Friend, R. H.; Gymer, R. W.; Holmes, A. B.; Burroughes, J. H.; Marks, R. N.; Taliani, C.; Bradley, D. D. C.; Dos Santos, D. A.; Brédas, J. L.; Lögdlund, M.; Salaneck, W. R. *Nature (London)* **1999**, *397*, 121.
- (2) Shin, C.-K.; Lee, H. *Synth. Met.* **2004**, *140*, 177.
- (3) Bao, Z.; Dodabalapur, A.; Lovinger, A. J. *Appl. Phys. Lett.* **1996**, *69*, 4108.
- (4) Sirringhaus, H.; Brown, P. J.; Friend, R. H.; Nielsen, M. M.; Bechgaard, K.; Langeveld-Voss, B. M. W.; Spiering, A. J. H.; Janssen, R. A. J.; Meijer, E. W.; Herwig, P.; de Leeuw, D. M. *Nature (London)* **1999**, *401*, 685.
- (5) Yu, G.; Gao, J.; Hummelen, J. C.; Wudl, F.; Heeger, A. J. *Science* **1995**, *270*, 1789.
- (6) Yang, X.; Loos, J.; Veenstra, S. C.; Verhees, W. J. H.; Wienk, M. M.; Kroon, J. M.; Michels, M. A. J.; Janssen, R. A. J. *Nano Lett.* **2005**, *5*, 579.
- (7) Hamed, M.; Forchheimer, R.; Inganäs, O. *Nat. Mater.* **2007**, *6*, 357.
- (8) Dhawan, S. K.; Singh, N.; Venkatachalam, S. *Synth. Met.* **2002**, *129*, 261.
- (9) Chen, T.-A.; Wu, X.; Rieke, R. D. *J. Am. Chem. Soc.* **1995**, *117*, 233.
- (10) Huynh, W. U.; Dittmer, J. J.; Alivisatos, A. P. *Science* **2002**, *295*, 2425.
- (11) Goffri, S.; Müller, C.; Stingelin-Stutzmann, N.; Breiby, D. W.; Radano, C. P.; Andreasen, J. W.; Thompson, R.; Janssen, R. A. J.; Nielsen, M. M.; Smith, P.; Sirringhaus, H. *Nat. Mater.* **2006**, *5*, 950.
- (12) Babel, A.; Jenekhe, S. A. *Macromolecules* **2004**, *37*, 98350.
- (13) Arias, A. C.; Endicott, F.; Street, R. A. *Adv. Mater.* **2006**, *18*, 2900.
- (14) Pal, S.; Nandi, A. K. *Macromolecules* **2003**, *36*, 8426.
- (15) Pal, S.; Roy, S.; Nandi, A. K. *J. Phys. Chem. B* **2005**, *109*, 18332.
- (16) Liu, C.; Oshima, K.; Shimomura, M.; Miyauchi, S. *Synth. Met.* **2006**, *156*, 1362.
- (17) Prosa, T. J.; Winokur, M. J.; Moulton, J.; Smith, P.; Heeger, A. J. *Macromolecules* **1992**, *25*, 4364.
- (18) Ihn, K. J.; Moulton, J.; Smith, P. J. *Polym. Sci., Part B: Polym. Phys.* **1993**, *31*, 735.
- (19) Kline, R. J.; McGehee, M. D.; Kadnikova, E. N.; Liu, J.; Fréchet, J. M. J.; Toney, M. F. *Macromolecules* **2005**, *38*, 3312.
- (20) Kim, D. H.; Jang, Y.; Park, Y. D.; Cho, K. J. *J. Phys. Chem. B* **2006**, *110*, 15763.
- (21) Yang, H.; Shin, T. J.; Yang, L.; Cho, K.; Ryu, C. Y.; Bao, Z. *Adv. Funct. Mater.* **2005**, *15*, 671.
- (22) Puigmartí-Luis, J.; Laukhin, V.; Pino, Á. P. d.; Vidal-Gancedo, J.; Rovira, C.; Laukhina, E.; Amabilino, D. B. *Angew. Chem., Int. Ed.* **2007**, *46*, 238.
- (23) Borsenberger, P. M.; Bäessler, H. J. *J. Chem. Phys.* **1991**, *95*, 5327.
- (24) Goonesekera, A.; Ducharme, S. J. *Appl. Phys.* **1999**, *85*, 6506.
- (25) Veres, J.; Ogier, S. D.; Leeming, S. W.; Cupertino, D. C.; Khaffaf, S. M. *Adv. Funct. Mater.* **2003**, *13*, 199.
- (26) Hulea, I. N.; Fratini, S.; Xie, H.; Mulder, C. L.; Iossad, N. N.; Rastelli, G.; Ciuchii, S.; Morpurgo, A. F. *Nat. Mater.* **2006**, *5*, 982.
- (27) Stassen, A. F.; Boer, R. W. I. d.; Iossad, N. N.; Morpurgo, A. F. *Appl. Phys. Lett.* **2004**, *85*, 3899.
- (28) Arias, A. C.; MacKenzie, J. D.; Stevenson, R.; Halls, J. J. M.; Inbasekaran, M.; Woo, E. P.; Richards, D.; Friend, R. H. *Macromolecules* **2001**, *34*, 6005.
- (29) Munson-McGee, S. H. *Phys. Rev. B* **1991**, *43*, 3331.
- (30) Celzard, A.; McRae, E.; Deleuze, C.; Dufort, M.; Furdin, G.; Maréché, J. F. *Phys. Rev. B* **1996**, *53*, 6209.
- (31) Sandler, J. K. W.; Kirk, J. E.; Kinloch, I. A.; Shaffer, M. S. P.; Windle, A. H. *Polymer* **2003**, *44*, 5893.

MA071135T